The Two-Loop Tracking Strategy for Real-Time Multi-Antenna GNSS Receivers

Pedro A. Roncagliolo, Jorge Cogo, and Javier G. García
Laboratorio de Electrónica Industrial, Control e Instrumentación (LEICI),
Dto. Electrotecnia, Facultad Ingeniería, UNLP, La Plata, Argentina.
Emails: {agustinr, jorge.cogo, jgarcia}@ing.unlp.edu.ar

***Abstract*—A multi-antenna global navigation satellite system receiver accepts many radio-frequency inputs simultaneously. Then, many antennas can be deployed on a vehicle and the receiver can decide which one is useful for the reception of each satellite´s signal. As a consequence, navigation solutions can be obtained in more adverse conditions, but at the cost of an important increase of the receiver complexity. Particularly, tracking of the satellite signals is a challenging task in these receivers, especially when a variation in the vehicle´s attitude impose a change in the antenna used for a satellite signal reception. Carrier tracking is critical during these changes of antenna since the distance between them is larger than the signal wavelength. Thus, a direct antenna commutation can produce important tracking transients that degrade the navigation measurements, affect data demodulation, and can produce a loss of signal tracking. The strategy presented in this work allows the receiver to keep tracking during these antenna commutations avoiding the detrimental tracking transients. Since it is based on close-loop schemes, it is suitable for real-time receivers due to their low computational complexity. The proposed technique is tested in a simulated low-earth orbit satellite scenario assuming a constant change of attitude due to a roll movement along the orbit direction vector. It is shown that a four-antenna receiver using the proposed tracking strategy can properly track the satellites in view, in spite of the frequent antenna commutations imposed by the vehicle´s rotation.**

***Index Terms*—GPS; GLONASS; Antenna Radiation Pattern; Carrier Tracking Loops; Antenna Commutation.**

I. INTRODUCTION

Global navigation satellite system (GNSS) receivers allow the real-time computation of a vehicle´s position and velocity, generally referred as navigation solutions. For this purpose the receiver has to detect, track and demodulate at least four signals broadcasted from the satellites of the system constellation [1]. Currently, the two operative GNSS systems are the Global Position System (GPS), supported by the United States, and GLONASS developed by Russia that has been completely operational since 1995. Typical GNSS applications rely on a single antenna for satellite signals reception [2]. Since usual antenna radiation patterns are hemispherical, the antenna location in the vehicle must be properly chosen to maximize satellite visibility. Therefore, single-antenna receivers are useful only if the vehicle´s attitude does not depart significantly from their assumed values, as is often the case with cars, planes and ships. However, this is not the case for other applications where the vehicle´s attitude does change considerably, like during the flight of some satellites and rockets. Since vehicle dimensions are larger than the signal wavelength, the direct combination of multiple antennas creates interference patterns that preclude proper receiver operation. A multi-antenna receiver is required in these cases [3]. This kind of receiver can also be used for vehicle´s attitude determination [1], and currently they are also being proposed for usual GNSS applications because better interference and multipath mitigation techniques can be applied [4].

Direct sequence spread spectrum (DS-SS) signals are utilized in GNSS because they allow high time-resolution. Therefore, a correlation stage is needed at the receiver to despread them and obtain reasonable signal-to-noise ratios [1]. Tight code and carrier synchronization of the local replica is required to achieve the de-spreading. Typically, tracking loop schemes are adopted for code and carrier synchronization in real-time receivers due to their low computational complexity. We assume a multi-antenna receiver architecture where the signal from each antenna is correlated individually. The same code and carrier local replica is used for all the signals from different antennas when receiving a particular satellite signal, assuming the multi-correlator channel scheme of [4]. However, since the goal in this work is maximizing satellite visibility and not interference and/or multipath mitigation, the beamforming approach is not considered. Then, only the antenna that produces the highest signal-to-noise ratio will be used for the tracking of a given satellite.

Considering that the distance between the antennas deployed on a vehicle is in the order of meters and the carrier wavelength is approximately 0.2 meters, an antenna commutation can be unnoticed by a code loop but can severely affect a phase loop. The degradation caused by this effect to the GNSS satellite data demodulation and some techniques to cope with it has been recently reported on [5]. The sudden change in the input phase can be avoided if that phase difference can be properly measured before the commutation actually occurs. In this case, the radiation patterns of deployed antennas should have a significant overlapping to assure continuous satellite visibility under vehicle´s attitude changes. Then, there should be enough signal-to-noise ratio at the second best antenna to measure the phase difference accurately before the moment when this antenna becomes the best and the tracking loop should change its input and use the new signal. In this work, we propose to use an auxiliary carrier tracking loop to estimate the differences between the signals coming from

 ISBN: 978-1-61208-264-6

the best antenna and the second best one. In this way, the phase transient are completely avoided, the quality of phase measures preserved, and the data demodulation unaltered.

The rest of the paper is organized as follows. A digital model for the output of the correlation of the received GNSS signal from multiples antennas with the same code and carrier local replica is presented in Section 2. The proposed carrier tracking strategy is presented in Section 3. The proposed scheme is tested in a simulated low-earth orbit (LEO) satellite scenario in Section 4. The tracking transient effects found if a single carrier loop scheme is used, and their absence when the two-loop strategy is adopted, are verified. Finally, the conclusions and future work lines are given in Section 5.

II. Digital Measurements Model

Consider that N antennas have been deployed on a vehicle and connected to a multi-antenna GNSS receiver. According to the receiver architecture described in the previous section, the signal received at each antenna must be correlated with the same locally generated replica for each visible satellite. The complex correlations of the incoming signal at the i-th antenna, from a given satellite and for the k-th correlation interval of duration T, can be expressed as [1]

$$C_k^i = D_k \sqrt{T \left.\frac{C}{N_0}\right|_k^i} \operatorname{sinc}(\Delta f_k^i) R(\Delta \tau_k^i) e^{j(\pi \Delta f_k^i T + \Delta \theta_k^i)} + n_k^i \quad (1)$$

where $i = 1, ..., N$, $C/N_0|_k^i$ is the carrier power to noise power spectral density of the signal from antenna i, $\Delta\tau_k^i = \tau_k^i - \hat{\tau}_k$ is the code delay estimation error, $\Delta f_k^i = f_k^i - \hat{f}_k$ is the frequency estimation error, both assumed constant during the integration time, and $\Delta\theta_k^i = \theta_k^i - \hat{\theta}_k$ is the initial phase estimation error. The term n_k^i is a complex white Gaussian noise sequence with unit variance, assumed independent between antennas, $R(\cdot)$ is the code correlation function, and $\operatorname{sinc}(x) = \sin(\pi x)/(\pi x)$. This expression assumes that the binary data bits $D_k = \pm 1$ are the same in all the antenna signals –given the slow data rate, e.g., 50 bps for GPS– and that correlations are computed within the same bit period. This type of binary data modulation is present in the GPS and GLONASS civil signals and in the data components of composite modernized GNSS signals. Notice that the estimated values, which corresponds to the local-replica, are the same in the correlations of different antennas, and that the carrier power to noise power spectral density $C/N_0|_k^i$ is affected by the gain of each antenna according to the line-of-sight vector of the received satellite.

A. Phase Discrimination

After the acquisition process has been completed, i.e., in tracking conditions [1], code and frequency estimation errors are sufficiently small so that the functions $\operatorname{sinc}(\cdot)$ and $R(\cdot)$ can be approximated by 1. Hence, (1) becomes

$$C_k^i = I_k^i + jQ_k^i = D_k \sqrt{T \left.\frac{C}{N_0}\right|_k^i} e^{j\Delta\phi_i} + n_i \quad (2)$$

where we have defined $\Delta\phi_k^i = \phi_k^i - \hat{\phi}_k$, with $\phi_k^i = \pi f_k^i T + \theta_k^i$ and $\hat{\phi}_k = \pi \hat{f}_k T + \hat{\theta}_k$, to model the input and output of the digital carrier tracking loops [6].

The phase estimation error present in the signal of each antenna is obtained from the angle of the corresponding complex correlation. To avoid the effects of binary modulation, a two quadrant discriminator should be utilized. Then,

$$e_k^i = \tan^{-1}\left(\frac{Q_k^i}{I_k^i}\right) = \left[\Delta\phi_k^i + n_{\phi_k^i}\right]_\pi \quad (3)$$

where the notation $[\cdot]_\pi$ indicates that its argument is kept within the interval $(-\frac{\pi}{2}, \frac{\pi}{2}]$ by adding or subtracting π as many times as needed. The noise term $n_{\phi_k^i}$ has zero mean and a complicated probability distribution. However, for high $C/N_0|_k^i$ values, it can be approximated by a Gaussian distribution with zero mean and variance $1/(2TC/N_0|_k^i)$.

B. Carrier Tracking Loops

The phase error estimates obtained with (3) are ambiguous due to the periodic nature of the phase. This ambiguity is responsible of many of the non-linear behaviours present in phase locked loops (PLL). Due to these non-linearities the PLL can have very long lock-in times and low resistance to high dynamics, and therefore many GNSS receivers add a frequency locked loop (FLL) in a scheme called FLL-assisted-PLL [7]. In previous works we have proposed an alternative solution, called the unambiguous frequency aided (UFA) PLL [6]. In the UFA-PLL, the ambiguous phase discriminator values, e_k^i, are corrected by adding or subtracting an integer number of π. The corrected phase errors, u_k^i, are found such that the difference between two successive values is less than a quarter of a cycle in magnitude. Thus, starting with $u_0^i = e_0^i$, it must be hold that

$$u_k^i = e_k^i - I_\pi(e_k^i - u_{k-1}^i) \quad (4)$$

where $I_\pi(x) = x - [x]_\pi$ is like the integer part function, but with steps at the multiples of π. The obtained sequence of phase errors u_k^i has unambiguous values as long as the frequency error is lower than $1/(4T)$. We have also shown that the UFA-PLL has the same noise resistance, and so the same tracking threshold, that an equivalent FLL [8].

Through the rest of this work, the utilized carrier loop is the UFA-PLL shown in Figure 1 whose filter coefficients are $p_1 = C = 0.5$, $p_2 = 0.105$, and $p_3 = 0.0123$. For the correlation time, $T = 5$ms, the resulting PLL has an equivalent noise bandwidth of 75.6Hz. The two delays included in the loop model the real-time calculation of the correlations. One of them accounts for the time spent in the computation itself, and the second is present because the estimated values utilized to produce the local-replica used in the correlation have to be known before the calculations begin. That is, the estimated value $\hat{\phi}_k$ is obtained with the loop filter output of the $(k-1)$-th correlation interval, which in turn is calculated with the estimated value $\hat{\phi}_{(k-2)}$. The loop filter is optimized for the tracking of acceleration steps, which produces a quadratic ramp of phase at the loop input. This loop design has been implemented in experimental GPS receivers

 ISBN: 978-1-61208-264-6

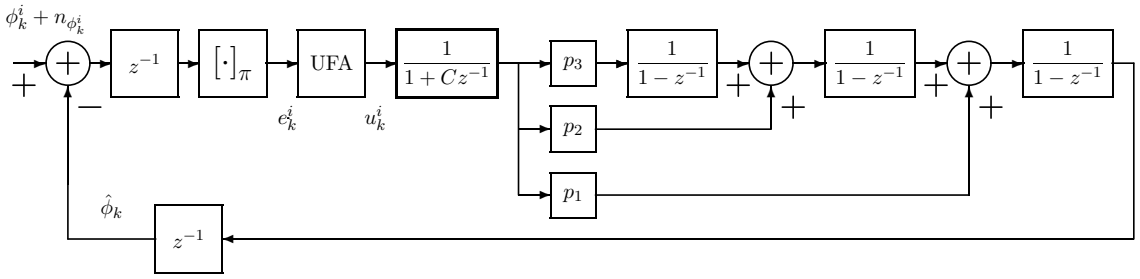

Fig. 1. Block diagram of the UFA-PLL model.

[6], and more details and properties can be found in [9]. The loop models previously described can be used operating data-bits synchronously as typically done, but can also be extended for data-bit asynchronous operation as proposed in [10].

III. The Two Loops Tracking Strategy

Assume the receiver is tracking a given satellite at the antenna l and that, due to the change in the vehicle´s attitude, the $C/N_0|_k^l$ values are decreasing and the $C/N_0|_k^j$ values, at the antenna j, are increasing. For the sake of simplicity, assume that the rest of the antennas has no useful signal levels. The correlations are computed based on the loop estimates computed with the signal from antenna l, but the error between the phase loop estimate and the phase of the signal from antena j can also be obtained as long as the $C/N_0|_k^j$ values are sufficiently high. This new phase error is

$$e_k^j = \tan^{-1}\left(\frac{Q_k^j}{I_k^j}\right) = \left[\Delta\phi_k^j + n_{\phi_k^j}\right]_\pi \qquad (5)$$

where $\Delta\phi_k^j = \phi_k^j - \hat{\phi}_k$. The phase error needed to build a new loop to track the signal from antenna j should be calculated with respect to a different phase estimate. However, if we assume that the frequency estimates from both loops are sufficiently close, the new phase error can be obtained from (5) by correcting it with the difference between both loop phase estimates. If we call $\hat{\phi}_k^M = \hat{\phi}_k$, the phase estimates of the actual loop or master loop, the phase error of an auxiliary loop, with phase estimate $\hat{\phi}_k^A$, is

$$eA_k^j = \left[e_k^j + \hat{\phi}_k^M - \hat{\phi}_k^A\right]_\pi = \left[\left[\Delta\phi_k^j + n_{\phi_k^j}\right]_\pi + \hat{\phi}_k^M - \hat{\phi}_k^A\right]_\pi$$

$$= \left[(\phi_k^j - \hat{\phi}_k^M + n_{\phi_k^j}) + \hat{\phi}_k^M - \hat{\phi}_k^A\right]_\pi = \left[\phi_k^j - \hat{\phi}_k^A + n_{\phi_k^j}\right]_\pi . \qquad (6)$$

The $[\cdot]_\pi$ operation is needed to obtain a phase error in the same range of values than the produced by a two quadrant inverse tangent. Notice that in the previous cases this operation was used to model the ambiguity of the measured phase error, but now it has to be actually implemented as part of the signal processing needed for the new auxiliary loop, which has input ϕ_k^j and output $\hat{\phi}_k^A$. The loop filter used for the auxiliary loop is exactly the same that the one used in the master loop. The reason for this choice will be clear in the following subsection.

A. Master Loop Actualization

Assume that the auxiliary loop has already been started and its initial transient, due to the initial phase and frequency errors, is already extinguished. Also assume that at the present moment the measured power at the antenna l becomes lower than the one at the antenna j. At this point the loop with the best estimates is the auxiliary one, and there is no reason to keep using the same loop estimates as parameters for the local-replica. Then, the master loop internal variables are overwritten by the ones from the auxiliary loop, and from now on its input is taken from the j antenna. In this way, the master loop is again tracking the best antenna, and the change has not produced any transient. Therefore, the logic for the master loop actualization is simple: each time that the power on the auxiliary loop becomes higher than the power on the master, the input of the master loop has to be changed by the auxiliary one. Depending on the auxiliary loop actualization logic, both loops can be tracking the signal from the same or different antennas. When both loops are tracking the signal from the same antenna no master loop actualization is possible, and the correction term of (6) becomes zero, and then $eA_k^j = eM_k^j$.

B. Auxiliary Loop Actualization

Now is clear that the aim of the auxiliary loop is to track the signal from the second best antenna whenever it is possible. Then, two possible situations have to be managed. The first is when the master loop is tracking the best antenna and the auxiliary one is properly tracking another antenna, which is not the second best antenna any more. That means that there is a better signal to be tracked with the auxiliary loop. Then, a direct commutation between these signals should be done at this loop. Of course, this change will produce a transient due to phase and frequency variations caused by the different physical locations and velocities of these antennas. However, since this loop is not generating the local-replica, the actual signal tracking will not be affected. The second situation is that the tracked signal in the auxiliary loop is actually the second best, but its power is too low to guarantee a satisfactory tracking. Then, the only possible option for the auxiliary loop is to switch its input to the same antenna that the master one. When this is the case, both loops should track the same signal until the second best antenna reaches a highly enough power level. At this point, the auxiliary loop should commute to this new antenna. Again, this change will cause a transient in the auxiliary loop, but it will not affect the master one.

 ISBN: 978-1-61208-264-6

TABLE I
ALGORITHMIC DESCRIPTION OF THE LOOP ACTUALIZATION.

if $P[a] > P[m]$ **then**
  $m \leftarrow a$
  Master loop variables $\leftarrow$ Auxiliary loop variables
end if
if $m = b$ **and** $P[s] > P[b]/10$ **then**
  $a \leftarrow s$
else
  $a \leftarrow b$
end if

C. Power Estimation

The strategy presented in this work needs a periodic estimation of the received power level for each satellite in view and for each antenna. This information can be obtained almost directly from the already computed correlations, (1), assuming that no interferences or severe signal obstructions or reflections are considered. A raw estimate of the received signal power from antenna i can be obtained as

$$\hat{P}_k^i = |C_k^i|^2 = (I_k^i)^2 + (Q_k^i)^2 = T \left.\frac{C}{N_0}\right|_k^i + noise \ . \quad (7)$$

Based on these values, better power estimates can be obtained by temporal filtering accordingly to the desired trade-off between noise reduction and the maximum rate of change of the filtered estimates, which is in turn established by the vehicle´s dynamics. One simple option is to take the average of each of these values during a selected time-window.

D. Summary of the Algorithm

A commutation period should be selected according to the expected vehicle´s dynamics, namely $L = KT$, with $K \in \mathbb{R}$. Then, every L seconds, a vector of estimated power at each antenna should be computed,

$$\bar{P} = [P[1]P[2] \cdots P[N]] \quad (8)$$

where each components is obtained as described in the previous subsection. Then, this vector has to be ordered and the two highest values and their corresponding indexes stored. If we called b the index of the first best antenna, and s to the index of the second best antenna, then $P[b] > P[s]$. Now consider that m and a are variables that indicate the number of the antenna selected for the master and the auxiliary loop respectively. Then, assuming that after the acquisition process of the satellite signal the loops are initialized with the best and the second best antenna at that moment, the algorithmic description –in pseudo code– of the proposed two loops tracking strategy is presented in Table I. In this code, it was considered that 10 dB less than the power of the signal in the master loop is the maximum difference allowed to the auxiliary loop to track a different signal.

IV. APPLICATION TO A LEO SATELLITE SCENARIO

In order to test the proposed tracking strategy, a LEO satellite scenario was simulated assuming a constant change of attitude due to a roll movement along the orbit direction vector of 5 revolutions per minute (rpm). This kind of rotation can be found during the first moments of the satellite life due to the spin stabilization used by the launching vehicles. In this case, the signals from the GNSS satellites can arrive from any direction. Then, the tetrahedron geometry shown in Figure 2 (a) was adopted for the placement of four antennas. The use of such non-aligned antenna array for this type of space application has been proposed in [11]. A typical GPS satellite constellation was considered and the position and velocity of each visible satellite were calculated. The same values were obtained for each antenna attached to the LEO satellite, whose trajectory is plotted in Figure 2 (b). Thirteen GPS satellites were found in view during some part of the 10 minutes of simulated trajectory. Notice that given the high velocity of the LEO satellite, $\simeq 7$ km/s, the time in view of a GPS satellite is much shorter than the found in earth applications. Based on the position and velocity values obtained, line-of-sight vectors, distances, and rate of change in these distances were computed every 10 ms to generate the input signals for the following digital processing. The change of the power level received at each antenna is a critical aspect in this analysis and therefore a realistic radiation pattern was considered. Since the GPS signals are radiating using right-handed circularly-polarized (RHCP) signals, the gain pattern of a typical patch antenna at the GPS L1 band (1575 MHz) was considered. The antenna gain pattern adopted is shown in Figure 2 (c).

A. Carrier tracking loop simulation

The loop simulations made are based on the correlation output model of (1). Then, the inputs required for each antenna and visible satellite are the carrier power to noise power spectral density, $C/N_0|_k^i$, the instantaneous carrier frequency f_k^i and the instantaneous input phase, θ_k^i. Since the code loops are not considered in this work, perfect code estimation is assumed. Neglecting second order terms, the instantaneous phase of the received signal can be obtained directly dividing the distance from the GPS satellite to the considered receiver´s antenna by the carrier wavelength, which is $\lambda \simeq 19$ cm for the GPS L1 frequency. In the same way, the frequency changes can be obtained considering only the Doppler effect, i.e., dividing the rate of change of the distance by λ. Finally, the gain factor G_{RHCP}, obtained with the line-of-sight vector and the gain pattern of the antennas, is converted into carrier power to noise power spectral density, according to

$$C/N_0|_k^i[dB] = G_{RHCP}[\text{dB}] + 42[\text{dB/Hz}] \quad (9)$$

where the value 42 dB/Hz, was obtained considering 2 dB of antenna losses, equivalent noise temperature of the antenna 130K, cable losses of 0.4dB and receiver noise figure of 1 dB.

B. Simulation results

The results presented in the first place correspond to a single loop tracking strategy. It simply consists on changing the loop input each time that the receiver detects that a better signal is available from another antenna. Only the results obtained with the tracking of one of the GPS satellites in view are presented due to space limitations. In Figure 3 (a), the C/N_0

 ISBN: 978-1-61208-264-6

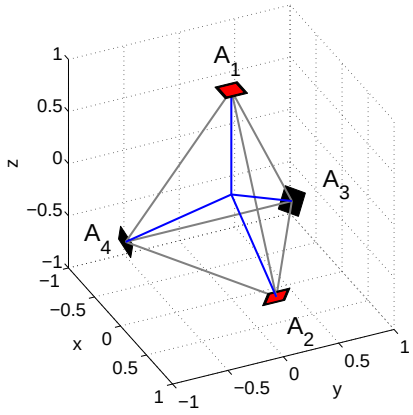

(a) Four antenna geometry on the LEO satellite.

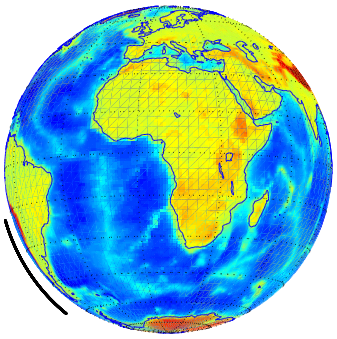

(b) Simulated LEO satellite trajectory.

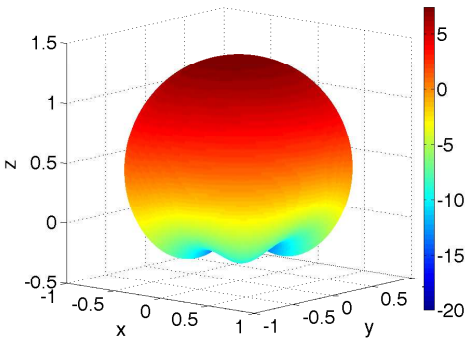

(c) Radiation pattern of a single antenna. RHCP gain in dB.

Fig. 2. Main elements of the simulated scenario.

levels of the signals received with each of the four antennas are plotted, for the first 30 seconds of the simulation, together with the indication of which antenna was used as input to the loop. A time-window of 0.25 seconds was selected for the power estimation average. The correct antenna selection made based on this power estimates, and the delay imposed by the averaging process can be clearly appreciated. The phase and frequency errors of the loop are presented in Figures 3 (b) and (c). Besides the first transient caused by the loop initialization, it can be clearly noticed the presence of a phase and frequency transients caused by the loop input commutations. Notice that half-cycle ambiguities present in the phase error were removed to appreciate the tracking error in a proper scale. These ambiguities can be easily compensated by the receiver, allowing continuous and reliable data demodulation.

The results obtained in the same situation but using the proposed two-loops tracking strategy are presented in Figure 4. In Figure 4 (a) the indication of the antennas selected as the input for the master and the auxiliary loops are plotted. It can be noticed that the master loop uses as input practically the same antenna that it would be used by the single loop. However, since its signal has been already tracked by the auxiliary loop, at the time of commutation the master loop can be properly initialized, and correspondingly a transient-free response is obtained as depicted in Figures 4 (b) and (c). Finally, it can be also appreciated that the estimation error levels change accordingly with the variation of the C/N_0 values of the tracked signal, as expected.

V. Conclusion and Future Work

An efficient tracking strategy devised for real-time multi-antenna GNSS receivers has been presented. The considered receiver architecture computes the correlations of the signal from each antenna with a common local-replica, for each tracked satellite. The use of a single carrier tracking loop in this kind of receiver will cause transient errors each time a commutation of the antenna used as loop input is done. These transients degrade the navigation measurements, affect data demodulation, and can produce a loss of signal tracking. The two-loop proposed strategy avoids these transients by properly modifying the internal loop variables at the moments of the commutations. The values of these variables are obtained by a second, twin loop, which does not require the calculation of extra correlations. The proposed strategy has been described in detail and tested in a simulated four-antenna LEO satellite scenario verifying that all the GPS satellites in view can be continuously tracked in the adverse situation of a rolling movement of 5 rpm.

The computational cost of the proposed strategy is minor assuming that in a multi-antenna receiver the power estimation and antenna selection algorithm is mandatory. Given the inherent increase of complexity of managing many radio-frequency inputs coherently, their digitalization, and the computation of the multi-correlations simultaneously, the cost of the extra loop seems negligible. The authors are now working on that multi-correlator architecture to be implemented in field programmable gate arrays (FPGA), and in the design of an experimental multi-antenna GNSS receiver.

VI. Acknowledgment

This work was funded by ANPCyT PICT 2011-0909 and UNLP 11-I-166.

References

[1] B. W. Parkinson and J. J. Spilker (eds.), *Global Positioning System: Theory and Applications*. Washington: American Institute of Aeronautics and Astronautics (AIAA), 1996.

[2] E. D. Kaplan, *Understanding GPS: Principles and Applications*. Boston: Artech House, 1996.

 ISBN: 978-1-61208-264-6

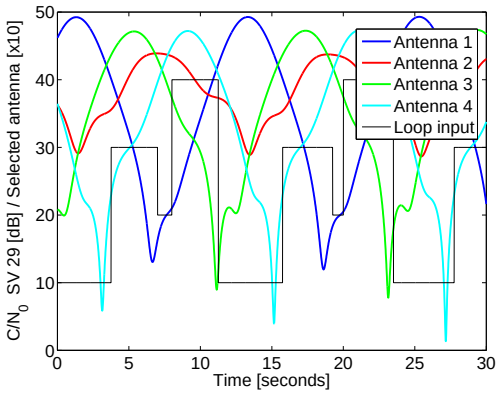

(a) C/N_0 values at each antenna and antenna selection.

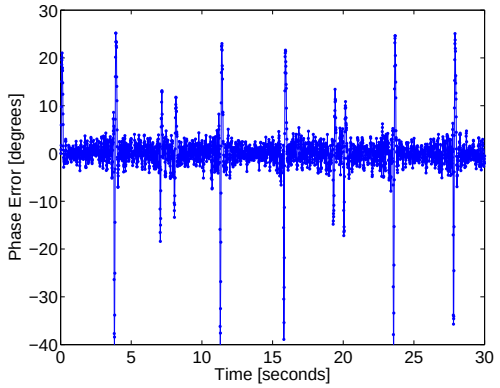

(b) Phase estimation error (commuted phase input).

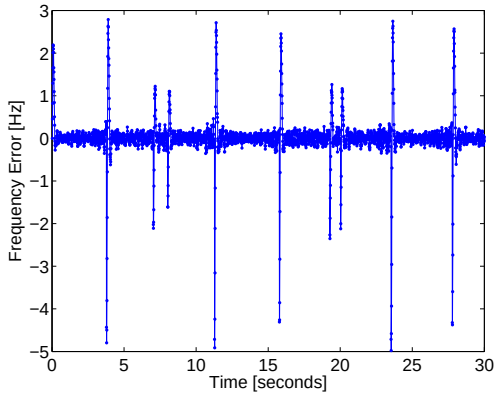

(c) Frequency estimation error (commuted frequency input).

Fig. 3. Tracking of SV 29 with a single loop strategy .

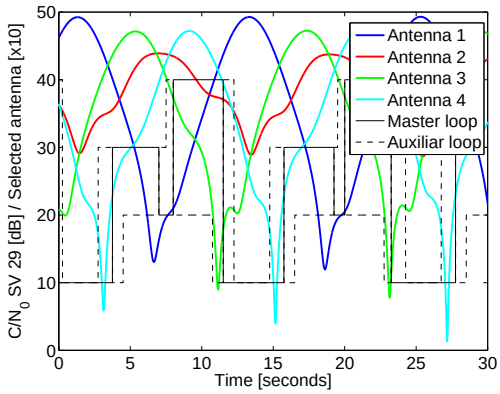

(a) C/N_0 values at each antenna and antenna selection.

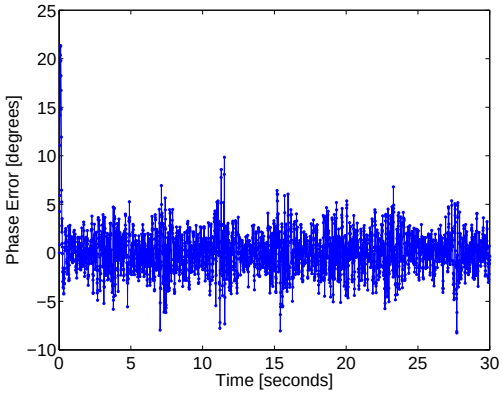

(b) Phase estimation error (commuted phase input).

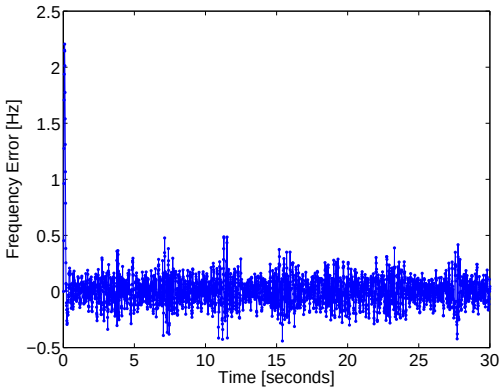

(c) Frequency estimation error (commuted frequency input).

Fig. 4. Tracking of SV 29 with the two loops strategy.

[3] T. Ebinuma, H. Saito, K. Tanaka, and T. Miyoshi, "GPS Signal Tracking on Spinning Vehicles with Antenna Diversity Techniques," in *Proccedings of ION GNSS 2009*, Savannah, GA, USA, September 2009, pp. 1413 – 1418.

[4] Kappen, G., C. Haettich, and M. Meurer, "Towards a Robust Multi-Antenna Mass Market GNSS Receiver," in *Proceedings of IEEE/ION PLANS 2012*, Myrtle Beach, SC, USA, April 2012, pp. 291–300.

[5] K. Harima, H. Saito, and T. Ebinuma, "Navigation Message Demodulation for GPS Receiver On-board Spinning Rockets," *GPS Solutions*, vol. 16, no. 4, pp. 495 – 505, October 2012.

[6] P. A. Roncagliolo and J. G. García, "High Dynamics and False Lock Resistant GNSS Carrier Tracking Loops," in *Proceedings ION GNSS 2007*, Fort Worth, TX, USA, September 2007, pp. 2364 – 2375.

[7] P. W. Ward, "Performance comparisons between FLL, PLL and a novel FLL-assisted-PLL carrier tracking loop under RF interference conditions," in *Proccedings of ION GPS 1998*, Nashville, TE, USA, September 1998, pp. 783 – 795.

[8] P. A. Roncagliolo, J. G. García, and C. H. Muravchik, "Pull-out Probability and Tracking Threshold Analysis for High Dynamics GNSS Carrier Loops," in *Proceedings of ION GNSS 2008*, Fort Worth, TX, USA, September 2008, pp. 221 – 228.

[9] P. A. Roncagliolo, J. G. García, and C. H. Muravchik, "Optimized Carrier Tracking Loop Design for Real-Time High-Dynamics GNSS Receivers," *Int. Journal of Navigation and Observation*, pp. 1–18, 2012.

[10] ——, "Data-Bits Asynchronous Tracking Loop Scheme for High Performance Real-Time GNSS Receivers," in *Proceedings of SPACOMM 2012*, Chamonix, France, April 2012, pp. 108 – 113.

[11] E. G. Lightsey, "Development and Flight Demonstration of a GPS Receiver for Space," Ph.D. dissertation, Department of Aeronautics and Astronautics, Stanford University, United States, Febraury 1997.

 ISBN: 978-1-61208-264-6